Voltage-Gated Sodium Channel Expression and Potentiation of Human Breast Cancer Metastasis

Scott P. Fraser,[1] James K.J. Diss,[1,2] Athina-Myrto Chioni,[1] Maria E. Mycielska,[1] Huiyan Pan,[1] Rezan F. Yamaci,[4] Filippo Pani,[1] Zuzanna Siwy,[7] Monika Krasowska,[7] Zbigniew Grzywna,[7] William J. Brackenbury,[1] Dimis Theodorou,[1] Meral Koyutürk,[5] Handan Kaya,[6] Esra Battaloglu,[4] Manuela Tamburo De Bella,[3] Martin J. Slade,[3] Robert Tolhurst,[3] Carlo Palmieri,[3] Jie Jiang,[3] David S. Latchman,[2] R. Charles Coombes,[3] and Mustafa B.A. Djamgoz[1]

Abstract

Purpose: Ion channel activity is involved in several basic cellular behaviors that are integral to metastasis (e.g., proliferation, motility, secretion, and invasion), although their contribution to cancer progression has largely been ignored. The purpose of this study was to investigate voltage-gated Na^+ channel (VGSC) expression and its possible role in human breast cancer.

Experimental Design: Functional VGSC expression was investigated in human breast cancer cell lines by patch clamp recording. The contribution of VGSC activity to directional motility, endocytosis, and invasion was evaluated by *in vitro* assays. Subsequent identification of the VGSC α-subunit(s) expressed *in vitro* was achieved using reverse transcription-PCR, immunocytochemistry, and Western blot techniques and used to investigate VGSCα expression and its association with metastasis *in vivo*.

Results: VGSC expression was significantly up-regulated in metastatic human breast cancer cells and tissues, and VGSC activity potentiated cellular directional motility, endocytosis, and invasion. Reverse transcription-PCR revealed that $Na_v1.5$, in its newly identified "neonatal" splice form, was specifically associated with strong metastatic potential *in vitro* and breast cancer progression *in vivo*. An antibody specific for this form confirmed up-regulation of neonatal $Na_v1.5$ protein in breast cancer cells and tissues. Furthermore, a strong correlation was found between neonatal $Na_v1.5$ expression and clinically assessed lymph node metastasis.

Conclusions: Up-regulation of neonatal $Na_v1.5$ occurs as an integral part of the metastatic process in human breast cancer and could serve both as a novel marker of the metastatic phenotype and a therapeutic target.

Breast cancer is the most common cancer of women and the second leading cause of female cancer mortality, accounting for about 10% of all cancer deaths in the western world (1, 2). To date, several breast cancer metastasis–associated genes have been identified both individually and in combination in microarray analyses (3, 4). These include oncogenes (e.g., *ras* and c-*myc*), cell cycle–associated markers (e.g., Ki67), adhesion molecules (e.g., E-cadherins), motility factors (e.g., hepatic growth factor), growth factors and their receptors (e.g., epidermal growth factor/Her-2 and fibroblast growth factor), and the well-established steroid hormones (e.g., estrogen and progesterone; refs. 3, 4). However, indirect measures of metastatic progression (including size of primary carcinoma, assessment of intratumoral vascular invasion, and lymph node involvement) remain the most widely used methods in clinical management. At present, although it is possible to detect micrometastases, approximately one third of women who seem disease-free at primary diagnosis eventually develop overt metastases (5, 6). Clinicians, therefore, require a more accurate diagnosis to predict the development of metastatic disease.

Ion channels are major signaling molecules expressed in a wide range of tissues where they have significant involvement in determining a variety of cellular functions: proliferation, solute transport, volume control, enzyme activity, secretion, invasion, gene expression, excitation-contraction coupling, intercellular communication, etc. (7). Consequently, ion channel defects

Authors' Affiliations: [1]Neuroscience Solutions to Cancer Research Group, Department of Biological Sciences, Imperial College London; [2]Medical Molecular Biology Unit, Institute of Child Health, University College; [3]Department of Cancer Medicine, CRC Laboratories, Medical Research Council Cyclotron Building, Imperial College School of Medicine, London, United Kingdom; [4]Department of Molecular Biology and Genetics, Bogazici University; [5]Department of Histology and Embryology, Kadir Has University; [6]Department of Pathology, Marmara University, Medical School, Istanbul, Turkey; and [7]Department of Physical Chemistry and Technology of Polymers, Silesian Technical University, Gliwice, Poland

Received 2/11/05; revised 4/13/05; accepted 4/18/05.

Grant support: Cancer Research UK (M.B.A. Djamgoz and R.C. Coombes); Breast Cancer Research Trust (M.J. Slade); Cancer Research Trust, KAV (M. Koyutürk); Medical Research Council, UK (W.J. Brackenbury); Pro Cancer Research Fund (M.B.A. Djamgoz, S.P. Fraser, and F. Pani); and Pro Cancer Research Fund Amber Fellowships (A-M. Chioni and H. Pan).

The costs of publication of this article were defrayed in part by the payment of page charges. This article must therefore be hereby marked *advertisement* in accordance with 18 U.S.C. Section 1734 solely to indicate this fact.

Note: S.P. Fraser and J.K.J. Diss contributed equally to this work.

Requests for reprints: Mustafa B.A. Djamgoz, Department of Biological Sciences, Imperial College London, Sir Alexander Fleming Building, South Kensington Campus, London SW7 2AZ, United Kingdom. Phone: 20-7594-54370; Fax: 20-7584-2056; E-mail: m.djamgoz@imperial.ac.uk.

(both genetic and epigenetic) are frequently an underlying cause of disease states (e.g., refs. 8–10). Ion channels, including voltage-gated ion channels (i.e., those activated by a change in membrane potential), could similarly have a significant role in cancer. Interestingly, electrodiagnosis has been practiced clinically, although its cellular/molecular basis remains unknown (11). We have shown previously that strongly metastatic human and rat prostate cancer cells express functional voltage-gated Na^+ channels (VGSC; refs. 12, 13). Importantly, VGSC activity contributes to many cellular behaviors integral to metastasis, including cellular process extension (14), lateral motility and galvanotaxis (15, 16), transverse invasion (12, 13, 17), and secretory membrane activity (18, 19). Consistent with this, (i) endogenous VGSC levels/activity were increased in a subline of the weakly metastatic LNCaP cells that exhibited significantly greater invasiveness and (ii) overexpression of VGSC alone was sufficient to increase *in vitro* cellular invasive potential, leading to the conclusion that VGSC activity is necessary and sufficient for cancer cell invasiveness (20).

Carcinomas of the breast and prostate share a number of similar features, including hormone sensitivity, a pronounced tropism for metastasis to bone and tendency for cooccurrence in families (21). A recent *in vitro* study has shown that the human MDA-MB-231 breast cancer cell line expressed functional VGSCs (22). However, both the molecular nature of the VGSC and its functional relevance to breast cancer *in vivo* are currently unknown. The present study aimed to determine (i) functional VGSC expression in breast cancer cell lines with a range of metastatic potential, (ii) whether VGSC activity contributed to cellular behaviors integral to metastasis, (iii) the molecular nature of the "culprit" VGSC(s), and (iv) whether VGSCα expression also occurred in breast cancer *in vivo* and correlated with metastasis.

Materials and Methods

Cell culture. MDA-MB-231, MDA-MB-468, and MCF-7 cells were grown in DMEM supplemented with 4 mmol/L L-glutamine and 5% to 10% fetal bovine serum. MCF-10A cells were grown in DMEM/Nut Mix F-12 supplemented with 4 mmol/L L-glutamine, 5% horse serum, 10 μg/mL insulin, 5 μg/mL hydrocortisone, 20 ng/mL epidermal growth factor, and 100 ng/mL cholera toxin.

Electrophysiology and pharmacology. Details of the patch pipettes, solutions, and the whole cell recording protocols were as described previously (12, 13, 23). Experiments on the cell lines were done on at least three separate dishes that had been in culture for 1 to 3 days. Further details are given in Fig. 1 legend. Tetrodotoxin was applied locally to individual cells by a puff pipette. All other compounds were bath applied.

Proliferation and toxicity assays. Proliferation was determined using the colorimetric 3-[4,5-dimethylthiazol-2-yl]-2,5-diphenyltetrazolium bromide assay (12). Results were obtained from eight separate experiments (each done in triplicate) with or without 10 μmol/L tetrodotoxin applied for 48 hours. Determination of tetrodotoxin toxicity was as described previously (14).

In vitro *assays.* Transwell assays were done with cells plated onto a 24-well cell insert with 12-μm pores at a density of 1.5×10^5 cells/mL, according to the manufacturer's instructions (BD Labware, Franklin Lakes, NJ). Cells were allowed to settle for 3 hours and treated appropriately for 7 hours. The number of cells migrating over 7 hours was determined using the 3-[4,5-dimethylthiazol-2-yl]-2,5-diphenyltetrazolium bromide assay (12). Results were compiled as the mean of eight repeats of drug versus control readings from individual dishes. Galvanotaxis was studied and variables determined as described previously (16). Endocytosis, employing horseradish peroxidase as a tracer, was done and effects quantified as described previously (18). Invasion assays were as before (12, 13) with cells plated at 2.5×10^5 cells per well in a chemotactic gradient of 1:10% fetal bovine serum. After 48 hours, invaded cells were quantified using 3-[4,5-dimethylthiazol-2-yl]-2,5-diphenyltetrazolium bromide.

***Reverse transcription-PCRs on breast cancer cells* in vitro.** Total cellular RNA was isolated from two batches of each of the cell lines by the acid guanidium thiocyanate-phenol-chloroform method (24). VGSCα degenerate primer screens were then done, as described previously (25) to identify the major VGSCαs expressed. Reactions designed to amplify specific VGSCαs were subsequently done on both strongly and weakly metastatic cell line extracts, using primer sequences and reaction annealing temperatures as described previously (25). VGSCα sequences were submitted to Genbank (accession nos. AJ310882-AJ310887 and AJ310896-AJ310900). Finally, semiquantitative PCRs based on kinetic observation of reactions were carried out as described previously (25) to determine relative VGSCα expression levels. NADH/cytochrome b5 reductase (hCytb5R) was used to control for the effects of variations in quality and quantity of the initial RNA, efficiency of the reverse transcription, and amplification between samples (25, 26).

"Neonatal" $Na_v1.5$ antibody. A polyclonal antibody (NESOpAb) was generated against a synthetic peptide with an amino acid sequence contained within the extracellular D1:S3 of neonatal $Na_v1.5$/VSE-NIKLGNLSALRC-NH_2. Four rabbits were immunized and antibody purified as described previously (27). The specificity of the antibody for the neonatal splice form of $Na_v1.5$ was validated on cell lines transfected with either neonatal or "adult" $Na_v1.5$ expression plasmids, by Western blotting, immunocytochemistry, and electrophysiology (28).

Immunocytochemistry and immunohistochemistry. Cells were plated on poly-L-lysine-coated coverslips for 48 hours. Paraformaldehyde fixation protocol was standard procedure. NESOpAb was used as the primary antibody. The secondary antibody was swine anti-rabbit conjugated to FITC (DAKO, Glostrup, Denmark). For immunohistochemistry, fresh-frozen or wax-embedded breast biopsies were prepared according to standard protocols. Primary antibody was NESOpAb. Secondary antibody was biotinylated swine anti-rabbit (DAKO). Avidin-biotin complex (DAKO) was then applied according to manufacturer's recommendation and the colour reaction was developed with a diaminobenzidine kit (Vector Laboratories, Burlingame, CA). Digital images were captured using Image-Pro Plus software (Media Cybernetics, Silver Spring, MD) and exported without further manipulation.

Reverse transcription-PCRs on breast biopsy tissues. Total cellular RNA was isolated from 0.1 to 0.5 g pieces of frozen tissue and single-stranded cDNA synthesized as above. Expression of $Na_v1.5$, $Na_v1.6$, and $Na_v1.7$ was then investigated by reverse transcription-PCR (RT-PCR), with hCytb5R reactions also done to control for the quality of the extracted RNA; samples which did not yield evident hCytb5R products were rejected unless UGSC expression was evident. RT-PCRs were carried out on each of at least two cDNA templates, manufactured independently from the same RNA extract. Sequences obtained from the human biopsies were submitted to Genbank (accession nos. AJ310888-AJ310895).

Epithelial cell purification. Epithelial cells were purified as described previously (29). Briefly, tissue was minced and digested in type IV collagenase in RPMI 1640 and 5% FCS, 2 mmol/L L-glutamine, 100 units/mL penicillin, 0.1 mg/mL streptomycin, 50 units/mL polymixin B, and 2.5 mg/mL amphotericin B until a single cell suspension was achieved. Undigested material was removed and redigested. Epithelial cells were purified and cultured in BCM [DMEM/F-12 (1:1) supplemented with 15 mmol/L HEPES, 2 mmol/L L-glutamine, 100 units/mL penicillin, 0.1 mg/mL streptomycin, 50 units/mL polymixin B, 2.5 mg/mL amphotericin B, 5 mg/mL insulin, 10 mg/mL apo-transferrin, 100 mmol/L ethanolamine, 1 mg/mL hydrocortisone, and 10 ng/mL epidermal growth factor] containing 10% FCS.

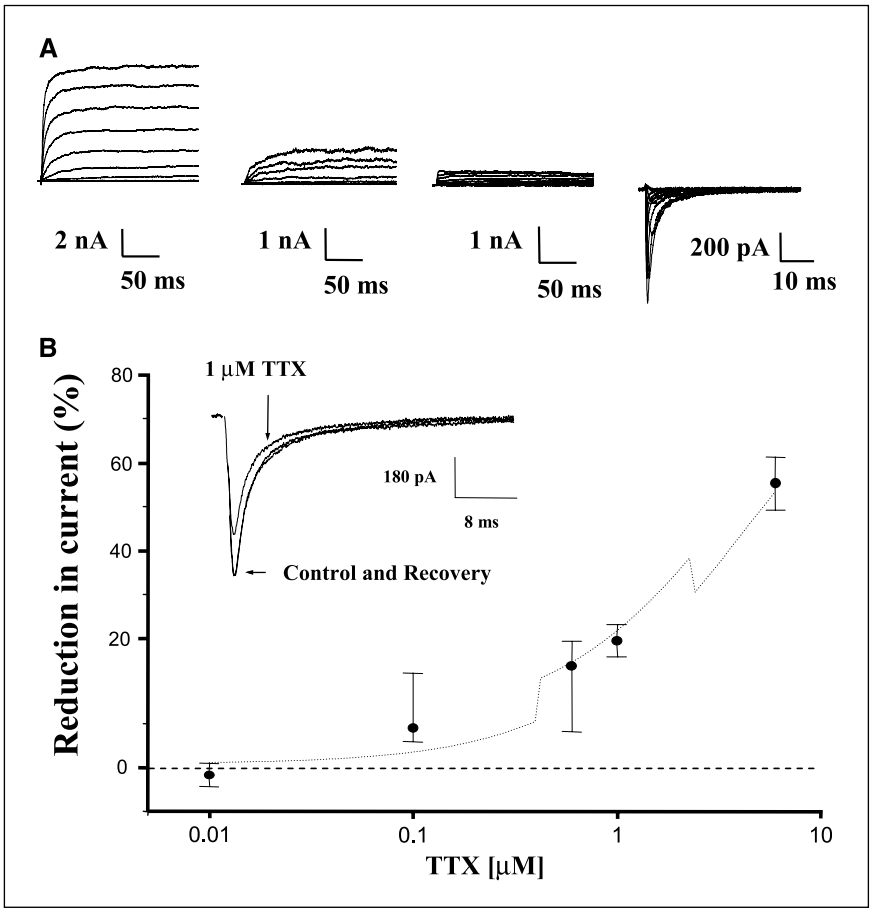

Fig. 1. Voltage-gated membrane currents in a human breast epithelial cell line and human breast cancer cells. *A,* voltage-gated membrane currents recorded in (*left* to *right*) MCF-10A, MCF-7, MDA-MB-468, and MDA-MB-231 cells. The currents were generated by pulsing the membrane potential from a holding voltage of −100 mV, in 5 mV steps, from −60 to +60 mV for 200 ms. Voltage pulses were applied with a repeat interval of 20 seconds. Every second current trace generated is displayed. *B,* dose-response curve for the effects of tetrodotoxin (*TTX*) on the VGSC current in MDA-MB-231 cells. The percentage reduction of the peak current at the fourth pulse (to −10 mV) following drug application was plotted as a function of drug concentration. Points, means of >5 different cells; bars, SE. Inset, a typical effect (and recovery) of one concentration of the drug on the inward current. *B,* the holding potential was −100 mV; the cell was pulsed repeatedly to −10 mV for 40 milliseconds every 20 seconds. The effect of tetrodotoxin was recorded from the fourth pulse following application.

Data analysis. All quantitative data were determined to be normally distributed and are presented as means ± SEs. Statistical significance was determined with Student's t test or χ^2 test, as appropriate. Results were considered significant at $P < 0.05$ (*).

Results

Functional voltage-gated Na^+ channel expression in breast cancer* in vitro: *electrophysiology and pharmacology. The essential electrophysiologic characteristics of a normal human breast epithelial cell line and three human breast cancer cell lines with a range of metastatic potentials were determined. Importantly, 70% of the strongly metastatic MDA-MB-231 cells tested (n = 69 of 99) expressed *inward* currents (representing influx of positive charge) activated by membrane depolarization (Fig. 1A). The inward currents were abolished in Na^+-free medium (data not shown), consistent with functional VGSC expression. In contrast, the normal breast epithelial cell line MCF-10A and the weakly metastatic MCF-7 and MDA-MB-468 breast cancer cells (n = 19-72) showed no inward currents (Fig. 1A). Membrane depolarization also activated *outward* currents (representing efflux of positive charge), which were reduced in line with increased metastatic potential in the cell lines studied (Fig. 1A, *left* to *right*). These currents were nearly completely (97%) abolished upon substituting Cs^+ for intracellular K^+ in MCF-7 cells, consistent with functional voltage-gated K^+ channel expression. Resting potentials in the normal extracellular bath medium were also inversely correlated with metastatic potential: MDA-MB-231 (−18.9 ± 2.1 mV), MDA-MB-468 (−31.1 ± 2.2 mV), MCF-7 (−39.9 ± 2.9 mV), and MCF-10A (−49.8 ± 2.6 mV; n = 9-27).

The VGSC currents in the MDA-MB-231 cells were suppressed by tetrodotoxin in a concentration-dependent manner with a concentration for half-blockage (IC_{50}) of 2.7 ± 0.5 μmol/L (n = 6; Fig. 1B), in agreement with functional expression of tetrodotoxin-resistant VGSCs. However, there was a small but consistent significant reduction (9 ± 3%; $P < 0.05$) in peak current with 100 nmol/L tetrodotoxin, indicating that a tetrodotoxin-sensitive VGSC was also present as a minor component (Fig. 1B). In addition, several clinically relevant antiarrhythmics and local anesthetics, as follows, blocked the VGSC currents with a range of potencies (IC_{50} values): flecainide (8.2 ± 1.3 μmol/L), mexiletine (11.0 ± 4.4 μmol/L), lidocaine (20.3 ± 3.0 μmol/L), procainamide (911 ± 163 μmol/L), and disopyramide (4,100 ± 200 μmol/L; n = 3-5).

***Contribution of voltage-gated Na^+ channel activity to metastatic cell behaviors* in vitro.** The possibility that functional VGSCs found in MDA-MB-231 cells contributed directly to metastatic behavior was examined using assays of (A) motility, (B) endocytosis, and (C) invasion (Fig. 2). These were measured in the presence and absence of tetrodotoxin (10 μmol/L) that would significantly (~80%) block VGSC activity but was nontoxic and did not affect cell proliferation. (A) Directional motility of the MDA-MB-231 cells was suppressed by tetrodotoxin (10 μmol/L). Transwell migration was reduced by 52% ($P < 0.01$; Fig. 2A1). A lower (200 nmol/L) concentration of

tetrodotoxin had no effect (data not shown). In addition, in a direct current electric field, the cells had an anodal occupancy of 94% and this was reduced to 56% following tetrodotoxin treatment, similar to control (i.e., nonfield) conditions (57%; Fig. 2A2). (B) Endocytosis, a measure of secretion and plasma membrane protein internalization, was also reduced by tetrodotoxin (47%) as well as by the removal of extracellular Na^+ (53%; $P < 0.05$ for both). However, the VGSC "opener" aconitine increased endocytosis by 14% ($P < 0.05$; Fig. 2B). (C) Finally, in a widely used *in vitro* assay of metastatic cell behavior, tetrodotoxin application inhibited Matrigel invasion of MDA-MB-231 cells by 49% ($P < 0.001$; Fig. 2C).

In contrast to the MDA-MB-231 cells, weakly metastatic MCF-7 cells were unable to migrate across transwell filters or invade through Matrigel and their galvanotactic motility and endocytic activity (both significantly weaker, compared with MDA-MB-231 cells) were unaffected by 10 μmol/L tetrodotoxin treatment (data not shown).

Molecular identity of breast cancer voltage-gated Na^+ channels in vitro. Using RT-PCR techniques, three VGSCαs were identified in both MDA-MB-231 and MCF-7 cells: $Na_v1.5$ (tetrodotoxin resistant), $Na_v1.6$ and $Na_v1.7$ (both tetrodotoxin sensitive; Fig. 3A). The overall level of VGSCα expression was much higher (>100-fold) in MDA-MB-231 compared with MCF-7 cells (Fig. 3B). This higher expression level was primarily due to $Na_v1.5$ (~1,800-fold greater expression in MDA-MB-231 cells), which constituted ~82% of the overall VGSCα mRNA expression in strongly metastatic cells. $Na_v1.7$ levels, making up most of the remaining ~18%, were also relatively higher in MDA-MB-231 cells. This agrees with the functional VGSC expression specifically in MDA-MB-231 cells being mainly tetrodotoxin resistant. $Na_v1.6$ was expressed at relatively low levels, which were similar in both cell lines.

All three VGSCαs were present in multiple splice forms (Fig. 3C). Importantly, DNA sequencing revealed that $Na_v1.5$ and $Na_v1.7$ were present predominantly in their D1:S3 5′-splice forms characterized by the absence at exon residue 7 of an aspartate (10). This form has previously been found in $Na_v1.1$-$Na_v1.3$, $Na_v1.6$, and $Na_v1.7$. The present study is the first to identify the existence of a D1:S3 5′-splice form of $Na_v1.5$. This differs from the known D1:S3 3′-splice form at 31 nucleotides, resulting in seven-amino-acid substitutions in an extracellular region of the VGSCα protein (Fig. 3D). All other VGSCα D1:S3 5′-splice forms differ from their D1:S3 3′ counterparts at just one to two amino acids.

Where examined, VGSCα D1:S3 5′-splice forms have previously been found to be expressed specifically in neonatal tissues (30, 31). We generated a novel D1:S3 5′-splice form–specific antibody and used it to verify that the D1:S3 5′-splice variant of $Na_v1.5$ was indeed neonatal (28). This was shown both by immunohistochemistry and Western blotting, comparing expression in neonatal and adult mouse cardiac muscle (where $Na_v1.5$ is abundant; Fig. 4A and B).

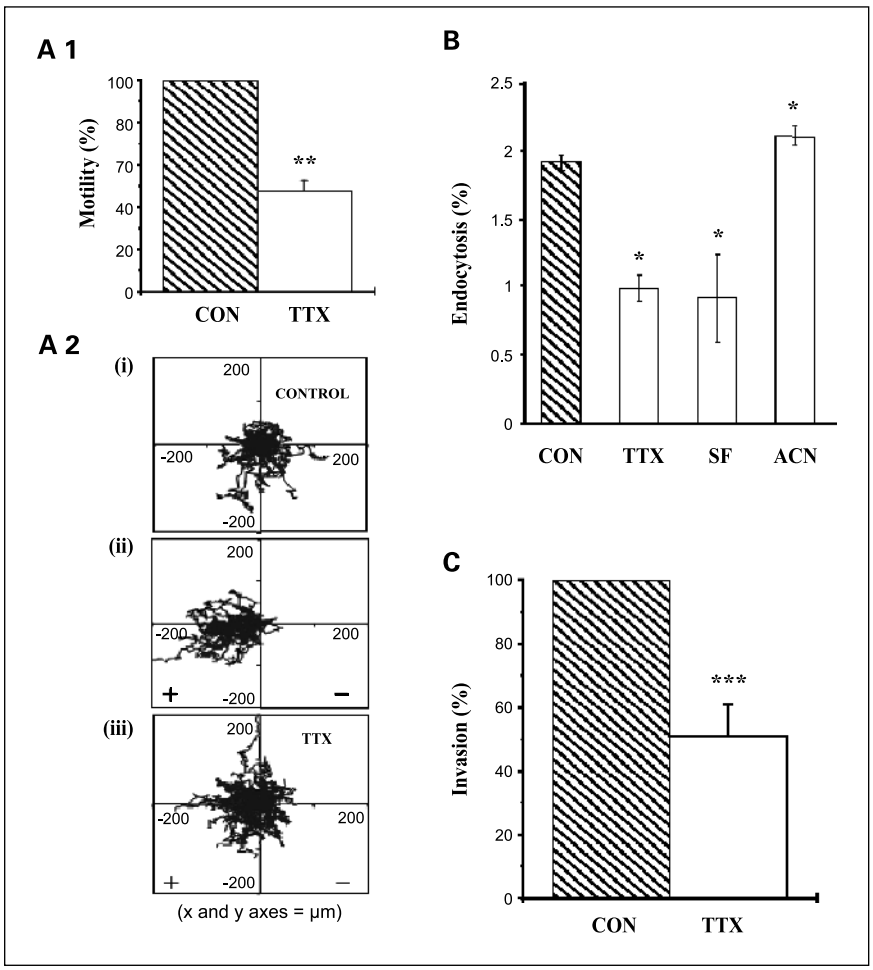

Fig. 2. *In vitro* evidence for VGSC involvement in metastatic MDA-MB-231 cell behaviors. *A1,* transwell motility data, normalized with respect to the control condition (*CON*, 100%) and following a 10-hour treatment with 10 μmol/L tetrodotoxin (*TTX*). *A2,* galvanotaxis. Superimposed trajectories of 50 cells are shown in each panel, the starting point being at the origin. i, control (no applied electric field); ii, electric field of 3 V/cm; iii, electric field of 3 V/cm with 10 μmol/L tetrodotoxin. *B,* endocytosis. Histobars, control (*CON*); 10 μmol/L tetrodotoxin (*TTX*); Na^+-free (*SF*); 400 μmol/L aconitine (*ACN*) treatments. *C,* Matrigel invasion. Each part details control conditions or following treatment with 10 μmol/L tetrodotoxin. *, $P < 0.05$; **, $P < 0.01$; and ***, $P < 0.001$, statistically significant differences.

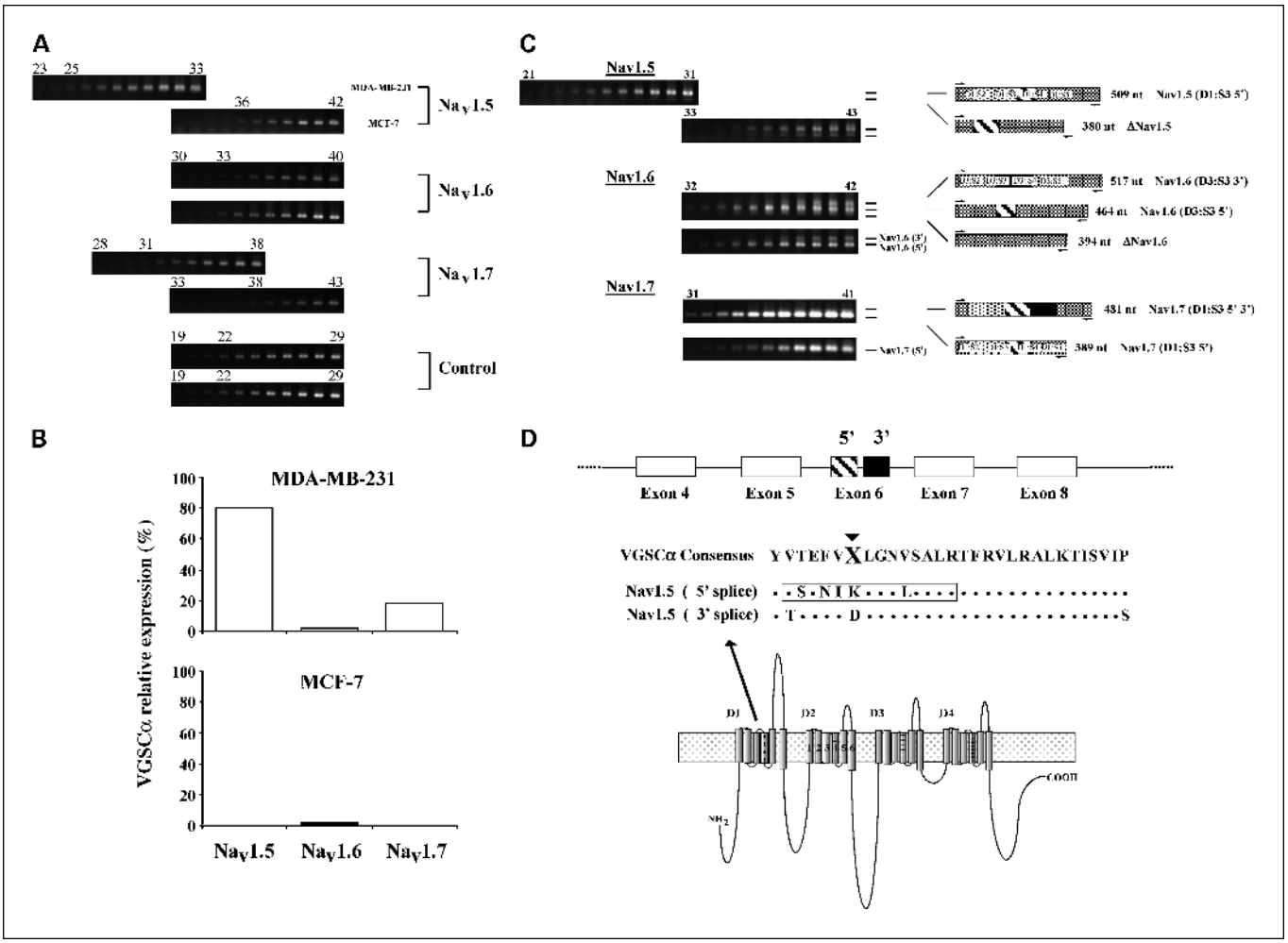

Fig. 3. Expression of VGSCα isoforms in breast cancer cells. *A,* semiquantitative PCR electrophoresis results for Na$_V$1.5, Na$_V$1.6, Na$_V$1.7, and hCytb5R controls done on MDA-MB-231 and MCF-7 cells. Representative PCR cycle numbers for given bands are indicated above the gels. Top, derived from MDA-MB-231 cell extracts; bottom, from MCF-7 extracts. *B,* proposed relative (%) expression levels of the three VGSCαs found to occur in the strongly (*white columns*) and weakly (*black columns*) metastatic cell lines. In each case, the vertical axis denotes the approximate level of expression with respect to total levels of expression of these three VGSCαs in the strongly metastatic MDA-MB-231 cells. Relative expression levels were estimated from degenerate screens and semiquantitative PCR data, taken together. *C,* details of the VGSCα splice forms expressed in the breast cancer cells. Gel images (*left*) and idealized bands representing each PCR product are indicated (*side, right*). 5′ and 3′ denote D1:S3 5′ (neonatal) and D1:S3 3′ (adult) alternatively spliced exons. Δ denotes forms with both alternatively spliced exons missing. *D,* Na$_V$1.5 D1:S3 5′ splice form amino acid data compared with the 3′ form and a VGSCα consensus sequence for this alternatively spliced exon. The 10 residue "neonatal-specific" sequence to which the neonatal Na$_V$1.5-specific antibody was generated is boxed. Location of adult/neonatal Na$_V$1.5 alternative splicing in the extracellular S3-4 linker of domain 1 is shown.

Furthermore, application of this antibody to the MDA-MB-231 and MCF-7 cells confirmed expression of the Na$_V$1.5 neonatal D1:S3 5′-splice form protein in the strongly metastatic cells specifically (Fig. 4C and D). Importantly, neonatal Na$_V$1.5 was present in the plasma membrane of the MDA-MB-231 cells, confirmed by Western blots on membrane fractions containing Glut-1, a specific marker of plasma membrane (Fig. 4D).

In vivo *expression of neonatal Na$_V$1.5 in human breast biopsy tissues.* Neonatal Na$_V$1.5 protein expression was markedly up-regulated in human breast cancer biopsy sections (n = 6), in comparison with normal human breast tissues (n = 4; Fig. 5A). Stained cells were of epithelial origin, as determined by MUC-1 immunoreactivity (not illustrated). Thus, the high level of neonatal Na$_V$1.5 protein expression found earlier in breast cancer *in vitro* also occurred *in vivo*. Expression of neonatal Na$_V$1.5 *in vivo* was further investigated by RT-PCR. In a "double-blind" test, expression of Na$_V$1.5 mRNA (but not Na$_V$1.6 nor Na$_V$1.7) in primary tumors was found to be strongly related to lymph node metastasis (LNM; Fig. 5B). The two characteristics were directly correlated in 14 of the 20 (70%) cases examined, being Na$_V$1.5$^+$/LNM$^+$ (n = 8) or Na$_V$1.5$^-$/LNM$^-$ (n = 6; χ^2 = 8.0; degree of freedom = 3; 0.05 > P > 0.01). There was no case of Na$_V$1.5$^-$/LNM$^+$; that is, metastasis to lymph nodes did not occur when Na$_V$1.5 was not detectable in the primary tumor. In a further case of a patient with bilateral breast cancer, Na$_V$1.5 expression matched the occurrence of respective LNM: Na$_V$1.5 was present in breast cancer with LNM (10 of 12) but absent from the contralateral breast with no LNM. Importantly, Na$_V$1.5 products were sequenced for 11 of the 14 Na$_V$1.5$^+$ cases and 10 (91%) were found to be the neonatal splice form. In addition, we were also able to readily detect neonatal Na$_V$1.5 mRNA expression in three of five epithelial cell populations purified from primary breast tumors (data not shown).

Discussion

The present study shows (i) that strongly but not weakly nor nonmetastatic breast cancer cells, displayed VGSC currents, mainly composed of a tetrodotoxin-resistant component; (ii) that blockage of the VGSC suppressed several metastatic cell behaviors *in vitro*; (iii) that a particular tetrodotoxin-resistant VGSCα, $Na_v1.5$, in its newly characterized neonatal splice form, was predominant in strongly metastatic cells; and (iv) that neonatal $Na_v1.5$ protein was markedly up-regulated in clinical breast cancer samples and that $Na_v1.5$ mRNA expression in biopsy samples correlated strongly with clinically assessed lymph node metastasis.

***Up-regulation of voltage-gated Na^+ channel activity and enhancement of metastatic cell behaviors* in vitro.** MDA-MB-231 cells expressed a functional VGSC that was predominantly tetrodotoxin resistant. Weakly metastatic/nontumorigenic cell lines did not express functional VGSCs. These results agree with the basic findings of Roger et al. (22). Importantly, the high-level VGSC expression was accompanied by much reduced outward currents in the MDA-MB-231 cell line. Although outward currents are known to play a role during the cell cycle in breast cancer cells (e.g., ref. 32), any significance of the reduction of the outward currents with increased metastatic potential in the cell lines studied remains to be investigated. Nevertheless, the specific combination of reduced outward and emergent VGSC inward currents would render these cells potentially more excitable in line with their "hyperactive" metastatic character.

The effectiveness of tetrodotoxin under resting conditions (in recordings and *in vitro* assays) would be consistent with VGSCs being tonically active in these cells. Indeed, Roger et al. showed there to be a "window current" between more than −60 and less than −20 mV, covering the prevailing resting membrane potential of approximately −19 mV. Furthermore, the concentration of tetrodotoxin (10 μmol/L) required to produce a functional effect was consistent with (a) $Na_v1.5$ being the VGSC underlying this behavior (at least in the *in vitro* migration assay where this was specifically tested) and (b) the patch-clamp pharmacology. The molecular mechanisms through which VGSC activity could potentiate directional motility, endocytosis, and invasion, could be direct and/or indirect. Direct effects could involve protein-protein interactions with cytoskeletal or extracellular matrix elements. Indeed, VGSCs physically associate, either via protein-binding domains in the major VGSCα or the auxillary VGSCβs, to ankyrin, contactin, neurofascin, and tenascin (33–37). In addition, $Na_v1.5$ is one of only two VGSCαs that has PDZ domains that could also enable cytoskeletal interactions. Indirect effects could involve a number of intracellular signaling mechanisms. In particular, changes in intracellular Na^+, Ca^{2+}, and/or H^+ could occur locally as a result of VGSC activity and lead to a variety of cellular effects that could contribute to metastasis. As well as

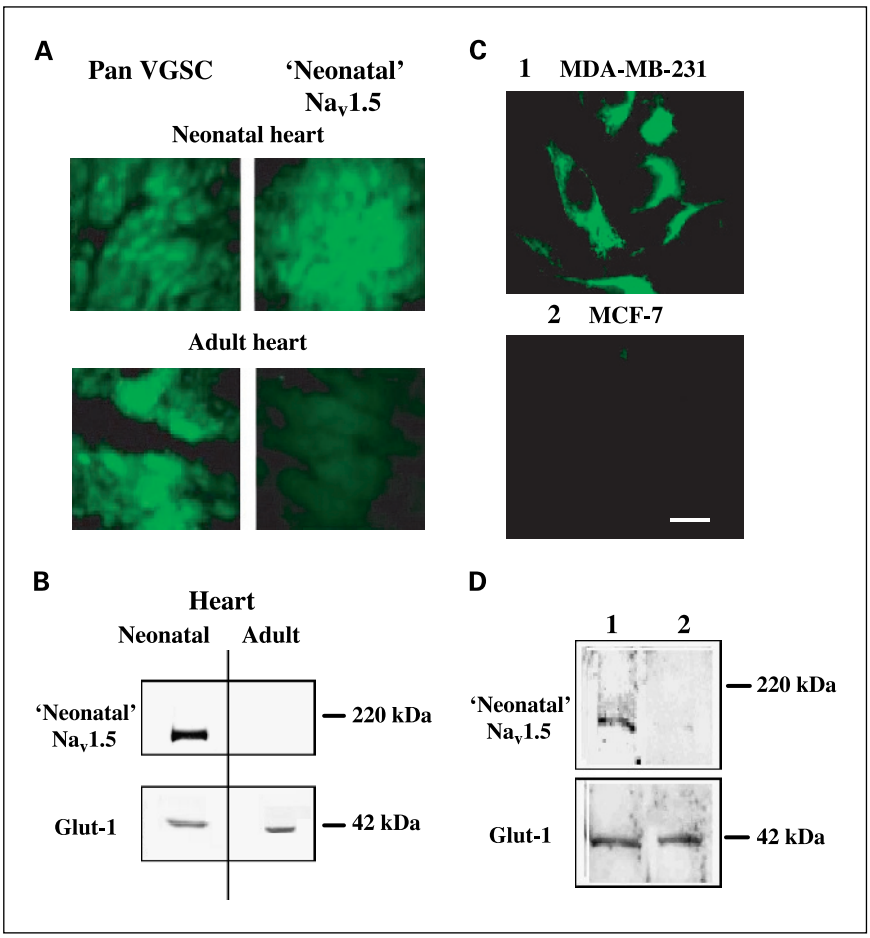

Fig. 4. Characterization of neonatal $Na_v1.5$ expression. *A,* immunohistochemical comparison of neonatal $Na_v1.5$ expression (as detected with the neonatal $Na_v1.5$-specific voltage-gated Na^+ channel antibody, NESOpAb) to "total" VGSC expression (as detected with a pan-specific VGSC antibody) in mouse heart from neonatal or adult tissue. *B,* Western blot data showing expression of neonatal $Na_v1.5$ in membrane fractions of neonatal but not adult mouse heart tissue. Membrane fractionation was confirmed through expression of the Glut-1 plasma membrane marker. *C,* representative images of the plasma membrane staining of (*1*) MDA-MB-231 but not (*2*) MCF-7 cells with NESOpAb. Negative controls gave no reaction (not illustrated). The cells were not permeabilized, because the antibody was raised to an extracellular epitope. *D,* Western blot data showing expression of neonatal $Na_v1.5$ (using NESOpAb) in membrane fractions of (*1*) MDA-MB-231 but not (*2*) MCF-7 cells. Membrane fractionation was confirmed through expression of the Glut-1 plasma membrane marker.

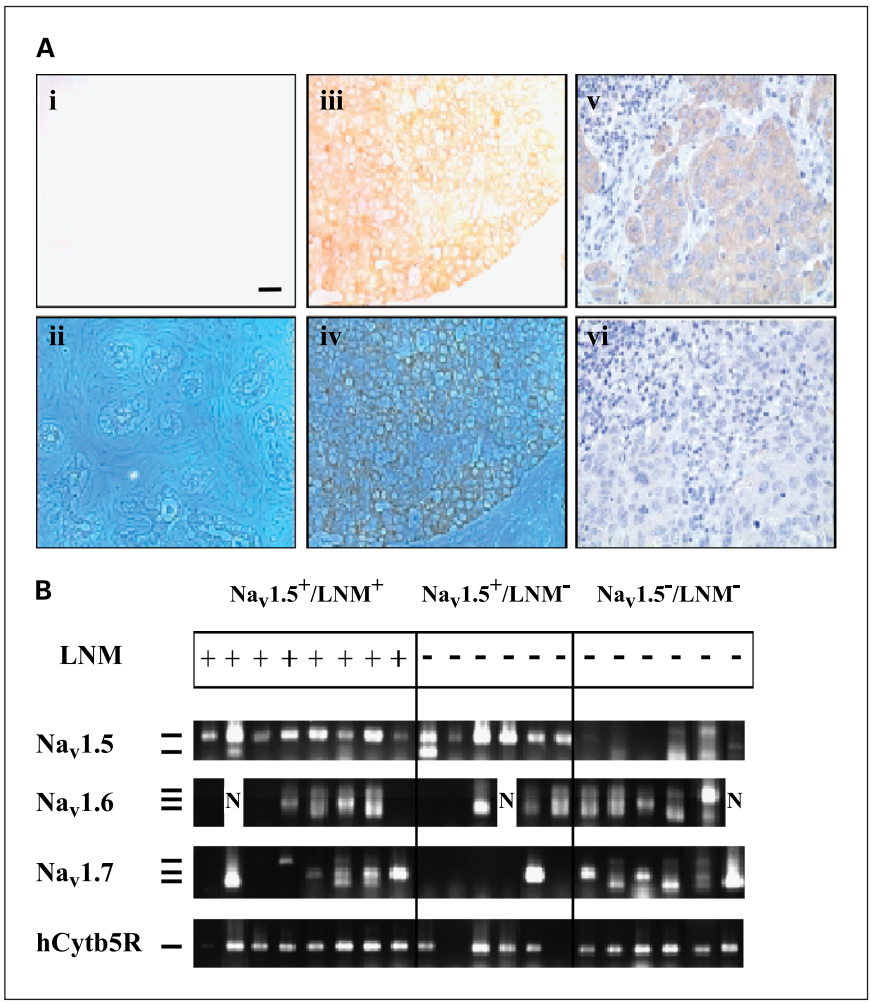

Fig. 5. Correlation of neonatal $Na_v1.5$ expression and breast cancer progression. *A,* immunohistochemical staining of human breast tissues with NESOpAb. Little staining was detected in normal human breast tissue as illustrated in (*i* and *ii*), whereas strong heterogeneous staining was detected in the corresponding image from breast cancer tissue (*iii* and *iv*). Bright field images of the sections (*i* and *iii*); corresponding phase-contrast images (*ii* and *iv*) to show the epithelial structure. The epithelial nature of the stained tissue was verified using an antibody raised against the epithelial marker MUC-1 (not illustrated). Controls done on H&E-stained breast biopsies by preabsorbing the primary antibody with the immunizing peptide did not yield evident staining (*vi*), in contrast to sections stained with NESOpAb (A_v). Bar, 50 μm. *B,* electrophoresis results of $Na_v1.5$, $Na_v1.6$, $Na_v1.7$, and hCytb5R control RT-PCRs done on 20 breast cancer tissue samples. LNM data for each sample are indicated above the gel images. Multiple bands corresponding to the evident splice form products (as previously described in Fig. 3 and ref. 25; *left*). PCRs were done for 55, 40, 40, and 30 cycles for $Na_v1.5$, $Na_v1.6$, $Na_v1.7$, and hCytb5R tests, respectively. (+), LNM was present; (−), LNM was not clinically evident.

effects upon motility and secretion, such changes could underlie more complex interactive functions such as gene expression, possibly in a feedback fashion (e.g., ref. 38).

***Up-regulation of neonatal $Na_v1.5$ voltage-gated Na^+ channel in metastatic breast cancer* in vitro.** RT-PCR showed that the predominant VGSCα expressed was $Na_v1.5$, in agreement with the mainly tetrodotoxin-resistant nature of the VGSC currents recorded. In fact, $Na_v1.5$ was expressed at ~1,000-fold higher levels in these strongly versus weakly metastatic cells. Regarding the other two minor VGSCαs expressed, $Na_v1.6$ was mainly present in its highly truncated "fail-safe" form and would not be functional (39). On the other hand, $Na_v1.7$ may account for the minor tetrodotoxin-sensitive component of the VGSC currents but its functional relevance, if any, it is not yet known.

Sequencing of $Na_v1.5$ PCR products revealed that $Na_v1.5$ transcripts predominantly possessed the D1:S3 5′ rather than the 3′ exon, being described here for the first time. For other VGSCαs with alternate D1:S3 forms, the 5′ exon is classically associated with neonatal expression (30, 31). Indeed, this was confirmed to also be the case for $Na_v1.5$ using a novel splice form-specific polyclonal antibody. Expression of the neonatal form of the culprit VGSC is consistent with the concept of oncofetal gene expression (e.g., refs. 40, 41). Nevertheless, it is not clear at this stage whether neonatal $Na_v1.5$ specifically is required for the proposed role of VGSC activity in breast cancer metastasis. Bennett et al. (20) have shown that invasion of human prostate cancer cells can be potentiated by the overexpression of a VGSCα ($Na_v1.4$) other than that normally predominant ($Na_v1.7$) in prostate cancer (25). Further work is required to elucidate whether neonatal $Na_v1.5$ is the only VGSCα subtype that can enhance metastastic cell behavior in breast cancer.

At present, the mechanism(s) responsible for the up-regulation of $Na_v1.5$ are not clear. Steroid hormones, especially estrogen, and growth factors (e.g., epidermal growth factor and fibroblast growth factor) are possible candidates, because breast epithelial tissue homeostasis and breast cancer onset/progression are under their strong influence. Epidermal growth factor has been shown to up-regulate VGSC functional expression (42–44). A functional association between fibroblast growth factor and $Na_v1.5$ has also been described (45). Importantly, the $Na_v1.5$ gene (*SCN5A*) core promoter has been characterized (46) and contains two putative estrogen receptor–binding ERE half-sites.[8]

Expression of neonatal $Na_v1.5$* in vivo: *clinical implications. Taken together, the *in vivo* data were highly consistent with

[8] J.K.J. Diss, unpublished analysis.

the *in vitro* findings regarding both increased VGSC expression with breast cancer progression (metastasis) and the molecular identity (neonatal $Na_v1.5$) of the candidate underlying VGSCα. The strong positive correlation between VGSCα expression and LNM in breast cancer biopsy tissue would suggest that VGSCs could act as an independent prognostic variable in a multivariant approach to this problem. Furthermore, the nature of involvement of VGSC activity in metastatic cell behavior is such as to make it likely that VGSC expression/up-regulation is an early event in the progression of breast cancer to the metastatic mode. The neonatal $Na_v1.5$ may also have therapeutic potential, in two main respects. First, the pharmacologic data indicated that neonatal $Na_v1.5$ was blocked by clinically important antiarrhythmics and local anesthetics; consistent with this, flecainide and mexiletine significantly inhibited endocytic activity in MDA-MB-231 but not MCF-7 cells (data not shown). Although not specifically tested here, it is possible that some such agents would block the neonatal form of the channel more than the adult and could thus be used clinically against metastatic breast cancer, with minimized side effects. Second, the antibody to the neonatal splice form of $Na_v1.5$ (recognizing an extracellular epitope) might itself be a novel, specific mechanism for targeting metastatic breast cancer in the adult (28). Interestingly, tamoxifen, a major anti-breast cancer drug, has been shown to strongly reduce VGSC activity (47, 48).

In conclusion, our results show that a novel neonatal splice form of $Na_v1.5$ is significantly up-regulated during breast cancer progression and potentiates a series of cell behaviors integral to the metastatic cascade. Accordingly, neonatal $Na_v1.5$ may have diagnostic and therapeutic potential in the clinical management of breast cancer.

References

1. Parkin DM, Pisani P, Ferlay J. Estimates of the worldwide incidence of 25 major cancers in 1990. Int J Cancer 1999;80:827–41.
2. Wingo PA, Ries LA, Rosenberg HM, Miller DS, Edwards BK. Cancer incidence and mortality, 1973–1995: a report card for the US. Cancer 1998;82:1197–207.
3. Schwirzke M, Schiemann S, Gnirke A, Weidle U. New genes potentially involved in breast cancer metastasis. Anticancer Res 1999;19:1801–14.
4. Van't Veer LJ, Dai HY, van de Vijver MJ, et al. Gene expression profiling predicts clinical outcome of breast cancer. Nature 2002;415:530–6.
5. Mansi JL, Gogas H, Bliss JM, et al. Outcome of primary-breast-cancer patients with micrometastases: a long-term follow-up study. Lancet 1999;354:197–202.
6. Heimann R, Hellman S. Clinical progression of breast cancer malignant behaviour: what to expect and when to expect it. J Clin Oncol 2000;18:591–9.
7. Hille B. Ionic channels of excitable membranes. 2nd ed. Sunderland (Massachusetts): Sinauer Associates Inc.; 1992.
8. Jurkat-Rott K, Lehman-Horn F. Human muscle voltage-gated ion channels and hereditary disease. Curr Opin Pharmacol 2001;1:280–7.
9. Viswanathan PC, Balser JR. Inherited sodium channelopathies: a continuum of channel dysfunction. Trends Cardiovasc Med 2004;14:28–35.
10. Diss JKJ, Fraser SP, Djamgoz MBA. Voltage-gated Na^+ channels: functional consequences of multiple subtypes and isoforms for physiology and pathophysiology. Eur Biophys J 2004;33:180–93.
11. Cuzick J, Holland R, Barth V, et al. Electropotential measurements as a new diagnostic modality for breast cancer. Lancet 1998;352:359–63.
12. Grimes JA, Fraser SP, Stephens GJ, et al. Differential expression of voltage-activated Na^+ currents in two prostatic tumour cell lines: contribution to invasiveness in vitro. FEBS Lett 1995;369:290–4.
13. Laniado ME, Lalani E-N, Fraser SP, et al. Expression and functional analysis of voltage-activated Na^+ channels in human prostate cancer cell lines and their contribution to invasiveness *in vitro*. Am J Pathol 1997;150:1213–21.
14. Fraser SP, Ding Y, Liu A, Djamgoz MBA. Tetrodotoxin suppresses morphological enhancement of the metastatic MAT-LyLu rat prostate cancer cell line. Cell Tissue Res 1999;295:505–12.
15. Fraser SP, Salvador V, Manning E, et al. Contribution of functional voltage-gated Na^+ channel expression to cell behaviours involved in the metastatic cascade in rat prostate cancer: I. Lateral motility. J Cell Physiol 2003;195:479–87.
16. Djamgoz MBA, Mycielska M, Madeja Z, et al. Directional movement of rat prostatic cancer cells in direct-current electric field: involvement of voltage-gated Na^+ channel activity. J Cell Sci 2001;114:2697–705.
17. Smith P, Rhodes NP, Shortland AP, et al. Sodium channel protein expression enhances the invasiveness of rat and human prostate cancer cells. FEBS Letts 1998;423:19–24.
18. Mycielska ME, Fraser SP, Szatkowski M, Djamgoz MBA. Contribution of functional voltage-gated Na^+ channel expression to cell behaviours involved in the metastatic cascade in rat prostate cancer: II. Secretory membrane activity. J Cell Physiol 2003;195:461–9.
19. Krasowska M, Grzywna ZJ, Mycielska ME, Djamgoz MB. Patterning of endocytic vesicles and its control by voltage-gated Na(+) channel activity in rat prostate cancer cells: fractal analyses. Eur Biophys J 2004;33:535–42.
20. Bennett ES, Smith BA, Harper JM. Voltage-gated Na^+ channels confer invasive properties on human prostate cancer cells. Pflugers Arch 2004;447:908–14.
21. Rodriguez C, Calle EE, Tatham LM, et al. Family history of breast cancer as a predictor for fatal prostate cancer. Epidemiology 1998;9:525–9.
22. Roger S, Besson P, Le Guennec J-Y. Involvement of a novel fast inward current in the invasion capacity of a breast cancer cell line. Biochim Biophys Acta 2003;1616:107–11.
23. Fraser SP, Grimes JA, Diss JKJ, Stewart D, Dolly JO, Djamgoz MBA. Predominant expression of Kv1.3 voltage-gated K^+ channel subunit in rat prostate cancer cell lines: electrophysiological, pharmacological and molecular characterisation. Pflugers Arch 2003;446:559–71.
24. Chomczynski P, Sacchi N. Single-step method of RNA isolation by acid guanidinium thiocyanate-phenol-chloroform extraction. Ann Biochem 1987;162:156–9.
25. Diss JKJ, Archer SN, Hirano J, Fraser SP, Djamgoz MBA. Expression profiles of voltage-gated Na^+ channel α-subunit genes in rat and human prostate cancer cell lines. Prostate 2001;48:165–78.
26. Fitzsimmons SA, Workman P, Grever M, et al. Reductase enzyme expression across the National Cancer Institute Tumor cell line panel: correlation with sensitivity to mitomycin C and EO9. J Natl Cancer Inst 1996;88:259–69.
27. Hermanson M, Funa K, Hartman M, et al. Platelet-derived growth-factor and its receptors in human glioma tissue - Expression of messenger-RNA and protein suggests the presence of autocrine and paracrine loops. Cancer Res 1992;52:3213–9.
28. Chioni A-M, Fraser SP, Pani F, et al. A Novel polyclonal antibody specific for the $Na_v1.5$ voltage-gated Na^+ channel "neonatal" isoform. J Neurosci Methods. In press.
29. Kothari MS, Ali S, Buluwela L, et al. Purified malignant mammary epithelial cells maintain hormone responsiveness in culture. Br J Cancer 2003;88:1071–6.
30. Sarao R, Gupta SK, Auld VJ, Dunn RJ. Developmentally regulated alternative RNA splicing of rat-brain sodium-channel messenger-RNAs. Nucleic Acids Res 1991;19:5673–9.
31. Gustafson TA, Clevinger EC, Oneill TJ, et al. Mutually exclusive exon splicing of type-III brain sodium channel-α subunit RNA generates developmentally-regulated isoforms in rat-brain. J Biol Chem 1993;268:18648–53.
32. Ouadid-Ahidouch H, Le Bourhis X, Roudbaraki M, et al. Changes in the K^+ current-density of MCF-7 cells during progression through the cell cycle: possible involvement of a h-*ether.a-gogo* K^+ channel. Receptors Channels 2001;7:345–56.
33. Srinivasan J, Schachner M, Catterall WA. Interaction of voltage-gated sodium channels with the extracellular matrix molecules tenascin-C and tenascin-R. Proc Natl Acad Sci U S A 1998;95:15753–7.
34. Xiao ZC, Ragsdale DS, Malhotra JD, et al. Tenascin-R is a functional modulator of sodium channel β subunits. J Biol Chem 1999;274:26511–7.
35. Malhotra JD, Kazen-Gillespie K, Hortsch M, Isom LL. Sodium channel β subunits mediate homophilic cell adhesion and recruit ankyrin to points of cell-cell contact. J Biol Chem 2000;275:11383–8.
36. Kazarinova-Noyes K, Malhotra JD, McEwen DP. Contactin associates with Na^+ channels and increases their functional expression. J Neurosci 2001;21:7517–25.
37. Ratcliffe CF, Westenbroek RE, Curtis R, Catterall WA. Sodium channel β1 and β3 subunits associate with neurofascin through their extracellular immunoglobulin-like domain. J Cell Biol 2001;154:427–34.
38. Itoh K, Stevens B, Schachner M, Fields RD. Regulated expression of the neural cell adhesion molecule L1 specific patterns of neural impulses. Science 1995;270:1369–72.
39. Plummer NW, McBurney MW, Meisler MH. Alternative splicing of the sodium channel SCN8A predicts a truncated two-domain protein in fetal brain and non-neuronal cells. J Biol Chem 1997;272:24008–15.
40. Ariel I, de Groot N, Hochberg A. Imprinted H19 gene expression in embryogenesis and human cancer: the oncofetal connection. Am J Med Genet 2000;921:46–50.

41. Monk M, Holding C. Human embryonic genes re-expressed in cancer cells. Oncogene 2001;20: 8085–91.
42. Toledo-Aral JJ, Brehm P, Halegoua S, Mandel G. A single pulse of nerve growth factor triggers long-term neuronal excitability through sodium channel gene induction. Neuron 1995;14:607–11.
43. Cota G, Meza U, Monjaraz E. Regulation of Ca and Na channels in GH3 cells by epidermal growth factor. In: Latorre R, Saez JC, editors. From ion channels to cell-cell conversations. NY: Plenum Press; 1977. p. 185–97.
44. Montano X, Djamgoz MBA. Epidermal growth factor, neurotropins and the metastatic cascade in prostate cancer. FEBS Letts 2004;571:1–8.
45. Liu CJ, Dib-Hajj SD, Renganathan M, et al. Modulation of the cardiac sodium channel Nav I.S by fibroblast growth factor homologous factor 1B. J Biol Chem 2003;278:1029–36.
46. Yang P, Kuperschmidt S, Roden DM. Cloning and initial characterization of the human cardiac sodium channel (SCN5A) promoter. Cardiovasc Res 2004; 61:56–65.
47. Smithermann KA, Sontheimer H. Inhibition of glial Na^+ and K^+ currents by tamoxifen. J Membr Biol 2001;181:125–35.
48. He J, Kargacin ME, Kargacin GJ, Ward CA. Tamoxifen inhibits Na^+ and K^+ currents in rat ventricular myocytes. Am J Physiol Heart Circ Physiol 2003;285: H661–8.

Article on Sodium Channels and Breast Cancer Metastasis

In the article on sodium channels and breast cancer metastasis in the August 1, 2005, issue of *Clinical Cancer Research*, the dose response curve in Fig. 1B was incorrectly represented. The correct Figure 1 appears below.

Fraser SP, Diss JKJ, Chioni A-M, et al. Voltage-gated sodium channel expression and potentiation of human breast cancer metastasis. Clin Cancer Res 2005;11:5381–9.

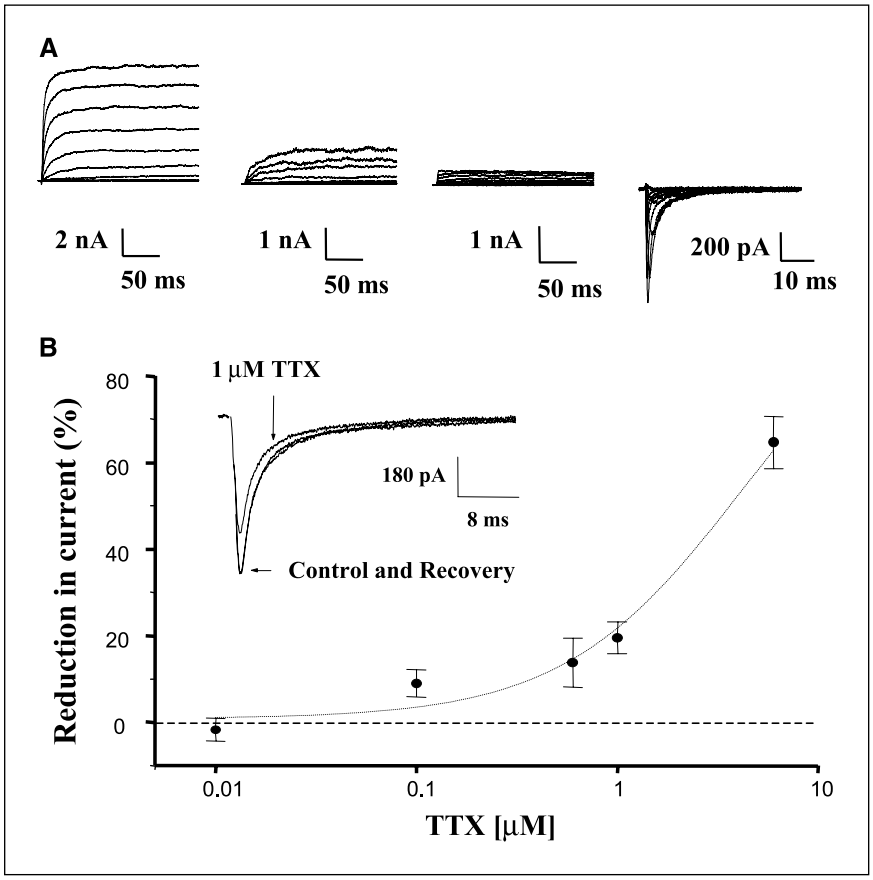

Fig. 1. Voltage-gated membrane currents in a human breast epithelial cell line and human breast cancer cells. *A,* voltage-gated membrane currents recorded in (left to right) MCF-10A, MCF-7, MDA-MB-468, and MDA-MB-231 cells. The currents were generated by pulsing the membrane potential from a holding voltage of −100 mV, in 5 mV steps, from −60 to +60 mV for 200 ms. Voltage pulses were applied with a repeat interval of 20 seconds. Every second current trace generated is displayed. *B,* dose-response curve for the effects of tetrodotoxin (*TTX*) on the VGSC current in MDA-MB-231 cells. The percentage reduction of the peak current at the fourth pulse (to −10 mV) following drug application was plotted as a function of drug concentration. Points, means of >5 different cells; bars, SE. Inset, a typical effect (and recovery) of one concentration of the drug on the inward current. *B,* the holding potential was −100 mV; the cell was pulsed repeatedly to −10 mV for 40 milliseconds every 20 seconds. The effect of tetrodotoxin was recorded from the fourth pulse following application.

Clinical Cancer Research

Voltage-Gated Sodium Channel Expression and Potentiation of Human Breast Cancer Metastasis

Scott P. Fraser, James K.J. Diss, Athina-Myrto Chioni, et al.

Clin Cancer Res 2005;11:5381-5389.